

Hemodynamic and Morphological Analysis of Mirror Aneurysms Prior to Rupture

This article was published in the following Dove Press journal:
Neuropsychiatric Disease and Treatment

Jinlong Yuan^{1,*}
Chenlei Huang^{2,*}
Niansheng Lai¹
Zhenbao Li¹
Xiaochun Jiang¹
Xuanzhi Wang¹
Xintong Zhao¹
Degang Wu¹
Jiaqiang Liu¹
Dayong Xia¹
Xinggen Fang¹

¹Department of Neurosurgery, The First Affiliated Hospital of Wannan Medical College (Yijishan Hospital), Wuhu, People's Republic of China; ²Department of Clinical Laboratory, The First Affiliated Hospital of Wannan Medical College (Yijishan Hospital), Wuhu, People's Republic of China

*These authors contributed equally to this work

Objective: Hemodynamic factors are thought to play important roles in the pathogenesis, progression, and rupture of cerebral aneurysms. Previous hemodynamic studies have been based on comparisons between post-ruptured and unruptured aneurysms. Nevertheless, changes of aneurysm morphology after rupture render these results unreliable. Moreover, pressure, age, gender, and the morphology of the parent artery also influence these results. Therefore, in the present study, we identified hemodynamic and morphological characteristics of aneurysms prior to rupture using twelve mirror aneurysms.

Materials and Methods: From our database, we retrospectively analyzed twelve mirror aneurysms (MANs) prior to rupture. Each mirror aneurysm was divided into the prior to rupture or the unruptured group. Patient-specific models were reconstructed from three-dimensional (3D) images of all patients. Hemodynamic and morphological factors were analyzed and compared.

Results: Compared with the unruptured side of MANs, aneurysms prior to rupture were significantly larger and significantly more irregular in shape; they also had significantly higher aspect ratio (AR), size ratio (SR), undulation index (UI), ellipticity index (EI), percentage of low wall shear stress area (LSA) and significantly lower normal wall shear stress (NWSS). The oscillatory shear index (OSI) and nonsphericity index (NSI) in the aneurysms prior to rupture were non-significantly higher than those of the unruptured group.

Conclusion: MANs prior to rupture may be extremely useful models to assess the risk of aneurysm rupture. Larger size, irregular shape, higher AR, SR, UI, NI, and lower WSS may be associated with aneurysms at risk for rupture.

Keywords: mirror aneurysms, computational fluid dynamics, hemodynamics, morphological, rupture

Introduction

With the development of neurovascular imaging technology and the introduction of family screening, a large quantity of asymptomatic unruptured aneurysms has been discovered.¹ The outcomes of aneurysm rupture are catastrophic; no matter how unruptured aneurysms were treated, whether by microsurgery or endovascular treatment, the potential risks are significant. For these reasons, it is difficult for neurosurgeons and to predict the risk of rupture of intracranial aneurysms (IAs), to identify high-risk patients, and to perform operations in a timely fashion.

The mechanisms of IA rupture are not understood well. Studies have demonstrated that hemodynamics plays an important role in the pathogenesis, progression, rupture of IA.¹⁻⁴ Nevertheless, hemodynamics might be affected by additional specific factors, including gender, collagen genetics, boundary conditions, vessel

Correspondence: Xinggen Fang
Email 18805536056@163.com;
xiady1981@163.com

morphology, blood pressure, and location.^{5,6} Mirror aneurysms (MANs), defined as intracranial bilateral saccular aneurysms at almost the same location on each side in the same patient, might weaken these influences. Initially, they occur in the same patient, probably proving an ideal internal control for variables such as blood pressure, age, gender and others.⁶⁻⁹ Moreover, because of MANs located in similar position on each side, they can eliminate the impact of the morphology of the parent artery on hemodynamics.⁶ In short, MANs help explore hemodynamic mechanisms of IA rupture. Studies based on patient-specific computational fluid dynamics (CFD) have compared hemodynamic and morphological characteristics between ruptured and unruptured aneurysms. Nevertheless, changes of aneurysm morphology caused by rupture events were ignored, contributing to the results of these studies being inaccurate.¹⁰⁻¹² A study of hemodynamic characteristics based on IAs prior to rupture might be more reasonable. Nevertheless, such a study would be constrained by ethical concerns. Therefore, in the present study, we performed hemodynamic and morphological analyses using twelve rare mirror IAs prior to rupture, with the aim of describing the relationship between hemodynamic characteristics and aneurysm rupture.

Materials and Methods

The Yijishan Hospital institutional review board approved this retrospective study. Written informed consent was acquired from all patients and the study was conducted in accordance with the Declaration of Helsinki.

Patient Selection

We retrospectively searched our aneurysm database for imaging data and medical records. Twelve patients with mirror aneurysms prior to rupture were found from December 2015 to December 2019. Inclusion criteria were as follows: 1) saccular MANs; 2) one aneurysm prior to rupture, and the other was unruptured; and 3) 3D digital subtraction angiography (DSA) images adequate for CFD analysis. Exclusion criteria were as follows: 1) fusiform or dissecting mirror aneurysms; 2) no aneurysm prior to rupture; and 3) 3D DSA images were too poor for CFD analysis. The aneurysms prior to rupture meant that the aneurysms ruptured within 7 days or there were unruptured posterior communicating artery (PComA) aneurysms with oculomotor nerve palsy (ONP). There were six patients diagnosed with unruptured mirror PComA aneurysms with ONP through DSA. The remaining six patients had mirror aneurysms, including one with PComA-MAN, three with ophthalmic artery aneurysms (OA-MANs) and with two middle cerebral artery aneurysms (MCA-MANs), suffering from subarachnoid hemorrhage (SAH) a few days after first being diagnosed using DSA. All clinical features are summarized in Table 1.

Imaging

3D images were obtained using digital subtraction angiography (Siemens, Artis Zee Floor VC14). Rotational angiograms were performed for 1-second after a 5-second contrast injection of a total of 15 mL contrast agent and 360° rotation, obtaining 266 frames. The corresponding 266 images were reconstructed on the Syngo X Workplace

Table 1 Clinical Features of Twelve Mirror Aneurysms Prior to Rupture

| No. | Age | Sex | HTN | DM | Smoking | Symptoms | Location | Days | Side | FUT |
|-----|-----|--------|-----|-----|---------|---------------------|----------|------|------|-----|
| 1 | 55 | Male | Yes | No | Yes | ONP | C7 | 3 | L | 3 |
| 2 | 46 | Female | No | No | No | ONP | C7 | 5 | R | 6 |
| 3 | 68 | Female | Yes | No | No | ONP | C7 | 5 | L | 8 |
| 4 | 70 | Male | No | Yes | No | ONP | C7 | 4 | R | 9 |
| 5 | 65 | Female | No | No | No | Headache | C7 | 3 | L | 12 |
| 6 | 58 | Male | No | No | Yes | ONP | C7 | 3 | R | 5 |
| 7 | 62 | Female | Yes | Yes | No | ONP | C7 | 2 | R | 6 |
| 8 | 57 | Male | Yes | No | Yes | Headache | C6 | 4 | L | 4 |
| 9 | 44 | Female | Yes | No | No | Episodic dizziness | C6 | 5 | R | 3 |
| 10 | 65 | Female | No | Yes | No | Headache, dizziness | C6 | 3 | R | 6 |
| 11 | 67 | Male | Yes | No | Yes | Incidental | MCA | 2 | L | 15 |
| 12 | 59 | Female | Yes | No | No | Headache | MCA | 4 | R | 6 |

Abbreviations: HTN, hypertension; DM, diabetes mellitus; L/R, left/right; ONP, oculomotor nerve palsy; Side, the location of aneurysm prior to the rupture of mirror aneurysm; FUT, follow-up time, the monitoring period of the unruptured one of mirror aneurysms; Days, interval time between hospitalization and subarachnoid haemorrhage or the interval time between onset of ONP and the DSA was performed; MCA, middle cerebral artery; The Bouthillier classification of internal carotid artery segments: C6, ophthalmic; C7, communicating.

workstation into 3D modeling that was then exported by stereolithography (STL) format. The pulsatile velocity waveform was obtained using transcranial Doppler from a healthy subject. We then captured the flow spectrum envelope to obtain average blood flow velocity waveform in a whole cardiac cycle using MATLAB 14.0 software (MathWorks, Natick, MA, US).

Patient-Specific Model

STL exported from the workstation was segmented and smoothed using GEOMAGIC STUDIO 12.0 (Geomagic, Morrisville, North Carolina). Then, the surface data were imported into ICEM CFD 14.0 (ANSYS, Canonsburg, Pennsylvania, US) to create volume grids for CFD simulations. The maximum element size was 0.3 mm and all surface data were meshed to create approximately 1 million finite volume tetrahedral element grids with four layers of prism elements for accurate calculation of WSS. The number of grids rarely affected simulation results when it was more than 1900 per cubic millimeter.¹³ The CFX 14.0 (ANSYS Inc., USA) was then used to solve the flow governing Navier-Stokes formulations with the assumption of laminar, incompressible, and Newtonian blood flow. The vessel wall was set as rigid wall with no-slip boundary condition. The density and dynamic viscosity of blood were assumed to be 1050 kg/m³ and 0.00345 Pa·s, respectively. Pulsatile velocity profile, derived from transcranial Doppler from a healthy individual, was applied for the inflow boundary condition. The flow waveforms were scaled to achieve a mean inlet WSS of 15 dyne/cm under pulsatile conditions.¹⁵ The outlet was set as opening boundary condition with zero static pressure. We discretized the whole cardiac cycle of 0.8 s by a time-step of 0.001 s for numeric simulation. Three cardiac cycles were simulated to acquire stable data, and the last cycle was taken as output.

Hemodynamic Parameter Calculation

Three hemodynamic parameters were calculated in this study: NWSS, percentage of low WSS area (LSA%), and OSI. NWSS was defined as WSS of aneurysm wall divided by WSS of the parent artery wall to allow comparisons among different patients.¹⁵ LSA% was defined as the areas of aneurysm wall exposed to the WSS below 1/10 of WSS of the parent artery wall, then normalized by the dome area.^{14,15}

Morphological Parameter Calculation

Eight morphological parameters, including aneurysm shape, size, aspect ratio (AR), size ratio (SR), undulation

index (UI), non-sphericity index (NSI), and ellipticity index (EI), were calculated. Aneurysm shape was classified as regular or irregular. Irregular shape was defined as aneurysms with bilobate blebs, polylobate blebs, or intra-aneurysmal thromboses.^{16,17} The other seven morphological parameters were described by Dhar et al.¹⁸

Statistical Analysis

The statistical analyses were performed using Microsoft Excel 2010 and SPSS11.0

(SPSS Inc, Chicago, Illinois). The Shapiro–Wilks *W*-test was used to determine whether a parameter was normally distributed. Data were presented as Mean ± SD (for normally distributed data) or median inter ± quartile range (for non-normally distributed data). The paired sample *t*-test (for non-normally distributed data) and nonparametric Wilcoxon test (for non-normally distributed data) were used to assess the statistical significance of all parameters between two groups. For qualitative data, the McNemar test was used to estimate the differences between the two groups. *P*-values < 0.05 were regarded as statistically significant.

Results

Patient Characteristics

There were seven females and five males with mean age 50.67 ± 7.94 years. The MANs included seven PComA-MANs, three OA-MANs (Figure 1: one of three OA-MANs), and two MCA-MANs. Eleven patients showed clinical symptoms and the remaining one was discovered incidentally. In terms of comorbidities, seven (58.3%) patients had hypertension and three patients (25%) had diabetes mellitus (DM). Four patients (33%) were smokers. Seven MANs were located on the right side and the remaining five were located on the left side. The follow-up time of unruptured aneurysms was at least three months (7.00 ± 3.45 months).

Morphological Parameters

The values of morphological parameters are summarized in Table 2. Compared with the unruptured group, the aneurysms prior to rupture (pr-ruptured) group was likely to have more irregular shape and there was a significant difference in aneurysm shape between the two groups.

The mean size of the pr-ruptured group was significantly larger than that of the unruptured group (8.25 vs 4.52 mm). Compared with the unruptured group, AR, SR, EI, UI were significantly higher in the pr-ruptured group.

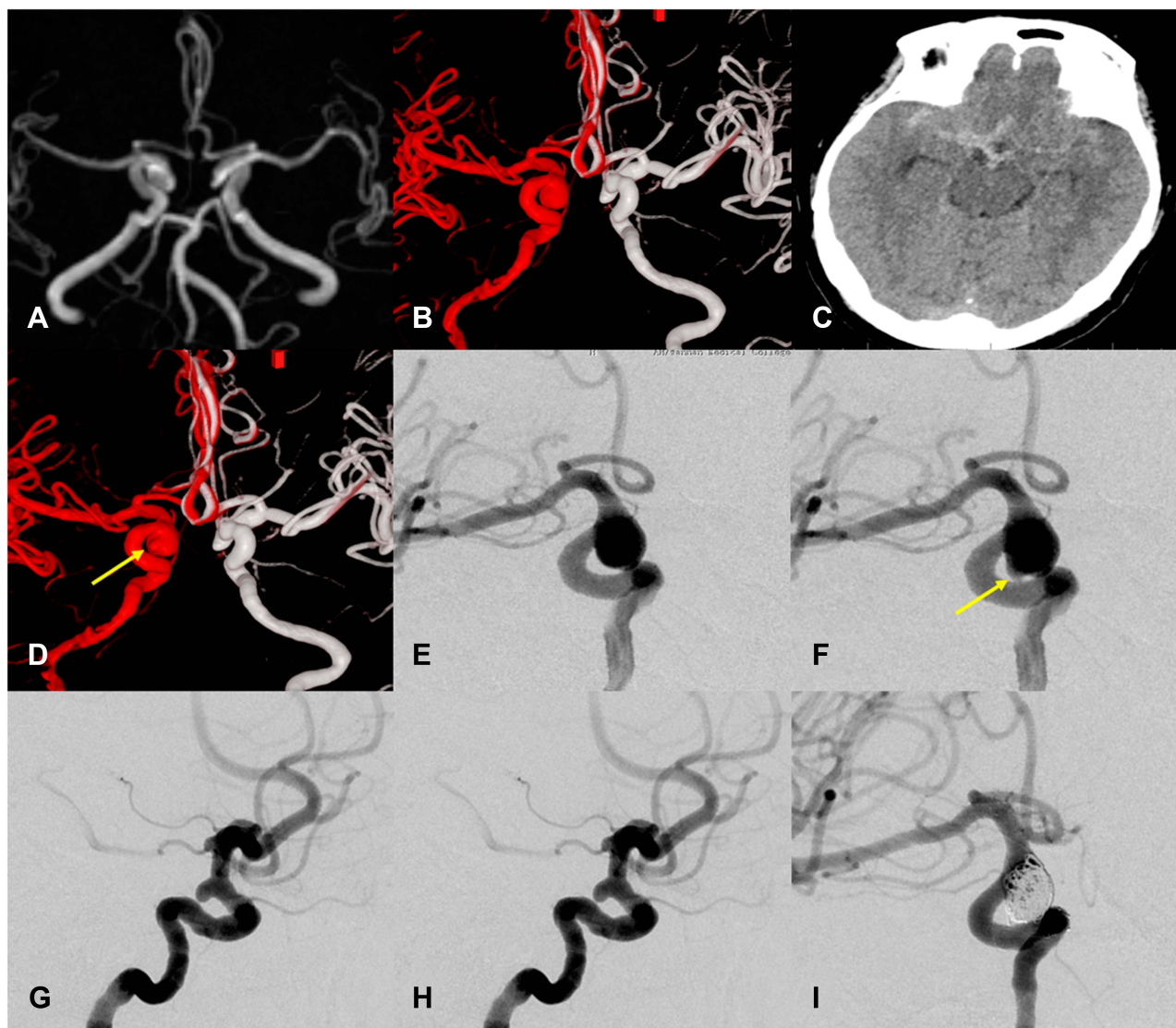


Figure 1 The images of a OA-MAN prior to rupture. A 44-year-old female presented with episodic dizziness. **(A)** Magnetic resonance angiography (MRA) shown a OA-MAN on the fifth day before rupture. **(B)** Dual fusion of 3D-DSA two days before rupture. **(C)** Brain CT scan revealed extensive SAH more on the right side on the fifth day after admission. **(D)** Dual fusion of 3D-DSA two days after rupture. **(E, F)** Morphological changes of the large right ophthalmic artery aneurysm prior to rupture. **(E)** Right internal carotid artery angiography revealed a large ophthalmic artery aneurysm before rupture. **(F)** Right internal carotid artery angiography of the large ophthalmic artery aneurysm after rupture indicated that the morphological became irregular (yellow arrow). **(G, H)** Left internal carotid artery angiography shown there was no change in the morphological of left unruptured ophthalmic artery aneurysm before **(G)** and after rupture **(H)**. **(I)** Angiogram obtained immediately after embolization revealed residual neck of the aneurysm.

NSI in the pr-ruptured group was non-significantly higher than that of the unruptured group (Table 2).

Hemodynamic Parameters

Twenty-four patient-specific CFD models for these 12 patients were reconstructed. The hemodynamic parameters are displayed in Table 2. The NWSS in the aneurysms prior to rupture group was significantly lower than that of unruptured aneurysms (Figure 2) and the WSS after rupture of the right ophthalmic artery aneurysm was relatively lower than WSS before rupture (Figure 3). By contrast, the LSA% in

the pr-ruptured aneurysms was significantly higher than that of unruptured aneurysms. OSI in the pr-ruptured group was non-significantly higher than that of the unruptured group.

Discussion

We first compared hemodynamic and morphological parameters between pr-ruptured aneurysms and unruptured aneurysms using twelve rare MANs prior to rupture. Larger size, irregular shape, higher AR, SR, UI, NI, and lower WSS were associated with the aneurysms prior to rupture.

Table 2 Results from Statistical Analysis of Hemodynamic and Morphological Parameters Examined in Mirror Aneurysms Prior to Rupture

| Parameters | Pr-ruptured ANs | Unruptured ANs | P-values |
|----------------|-----------------|-------------------|----------|
| Aneurysm shape | | | |
| Regular | 2(16.7%) | 9(75%) | |
| Irregular | 10(23.3%) | 3(25%) | 0.012 |
| Size | 8.25±2.95 | 4.52±0.62 | <0.001 |
| AR | 1.42±0.51 | 1.05±0.49 | 0.042 |
| SR | 2.60±0.81 | 1.81±0.42 | 0.003 |
| EI | 0.21±0.39 | 0.13±0.01 | 0.02 |
| UI | 0.19±0.08 | 0.048±0.025 | <0.001 |
| NSI | 0.20±0.35 | 0.18±0.52 | 0.091 |
| NWSS | 0.54±0.21 | 0.75±0.19 | <0.001 |
| LSA(%) | 0.16(0.12,0.25) | 0.02(0.003,0.063) | 0.002 |
| OSI | 0.026±0.009 | 0.023±0.010 | 0.136 |

Abbreviations: Pr-ruptured ANs, the aneurysms prior to rupture of mirror aneurysms; Unruptured ANs, unruptured aneurysms of the mirror aneurysms prior to rupture; AR, aspect ratio; SR, size ratio; EI, ellipticity index; UI, undulation index; NSI, non-sphericity index; NWSS, normalized WSS, the WSS-aneurysm wall divided by the WSS-parent artery; LSA%, percentage of low WSS area; OSI, oscillatory shear index.

ONP with the unruptured PComA, considered as sudden enlargement of the aneurysm sac, is a typical symptom warning for urgent treatment.^{19,20} Nearly all the neurosurgeons share the consensus opinion that unruptured PComA with ONP is prior to rupture. In addition, the unruptured aneurysms that eventually ruptured within 7 days after initial symptoms (headache, dizziness), were considered at high risk of rupture.¹²

Previous CFD studies based on neurovascular imaging have suggested that hemodynamics plays an important role in the pathogenesis, progression, rupture or stabilization of IA.¹⁻⁴ Nevertheless, most hemodynamic studies concentrated on the comparisons between ruptured and unruptured aneurysms and ignored the morphological changes of IAs after aneurysm rupture.²¹ This has fostered skepticism regarding the accuracy of these results.

Several case reports and controlled studies have described hemodynamic and morphological differences in IAs prior to rupture. Sforza et al first performed hemodynamic simulation of a terminal basilar tip aneurysm prior to rupture.¹¹ They showed that a concentrated inflow jet creating a small region of locally elevated WSS was associated with the aneurysm's rupture. Subsequently, at the same center, Cebra et al analyzed the hemodynamic parameters of a lethal basilar artery aneurysm just prior to rupture.¹² They reached the same conclusion as Sforza

et al Kono et al also presented a CFD study to show changes in aneurysm shape after rupture.¹⁰ These hemodynamic simulations of aneurysms prior to rupture suggest that these investigators paid attention to alterations in morphological parameters based on rupture events; they noted that hemodynamic analysis based on unruptured and ruptured aneurysms is a questionable approach.

Because the number of patients with aneurysms prior to rupture is small, three case-control studies were performed. Pereira et al performed a case-control study of four small IAs in terms of hemodynamics.²² Although the WSS in the patients was lower than those in controls, the differences were not statistically significant. Liu et al concluded that IA prior to rupture had lower WSS, higher AR, and more irregular shape in a case-control study of hemodynamics and morphology of three giant aneurysms.²³ Duan et al also concluded that posterior communicating aneurysms prone to rupture had higher LSA, lower WSS, and NWSS in a similar matched case-control study.²⁴ Multivariate conditional logistic regression analysis showed the WSS might be a more reliable factor associated with rupture of PComA. In the three case-control studies, the size, position or clinic records were regarded as matching factors, while the patient-special boundary conditions were ignored. The MANs disease model might circumvent this limitation.

MANs, defined as intracranial bilateral saccular aneurysms at almost the same location on each side in the same patient, accounted for approximately 20–30% among multiple aneurysms.^{25,26} Because the MANs disease model provides conditions in which most variables were equal, including gender, blood pressure, anatomic positions, morphological parameters of parent arteries, and collagen genetics, it was particularly helpful for setting of boundary conditions. While phase-contrast MR can offer patient-special boundary conditions, its accuracy also needs to be validated. Furthermore, as a retrospective study, it barely acquired every patient-specific boundary condition. Comparing the hemodynamic characteristics by adopting the MANs model, we might achieve more reasonable results.

The present study provides hemodynamic and morphological analysis using twelve rare MANs prior to rupture, eliminating influences of morphological change of IA after aneurysm rupture and circumventing the issue of setting of boundary conditions. We found that aneurysms prior to rupture have higher LSA% and lower NWSS. The result might be more accurate as well as according to the results of the three case-control studies mentioned above. The low

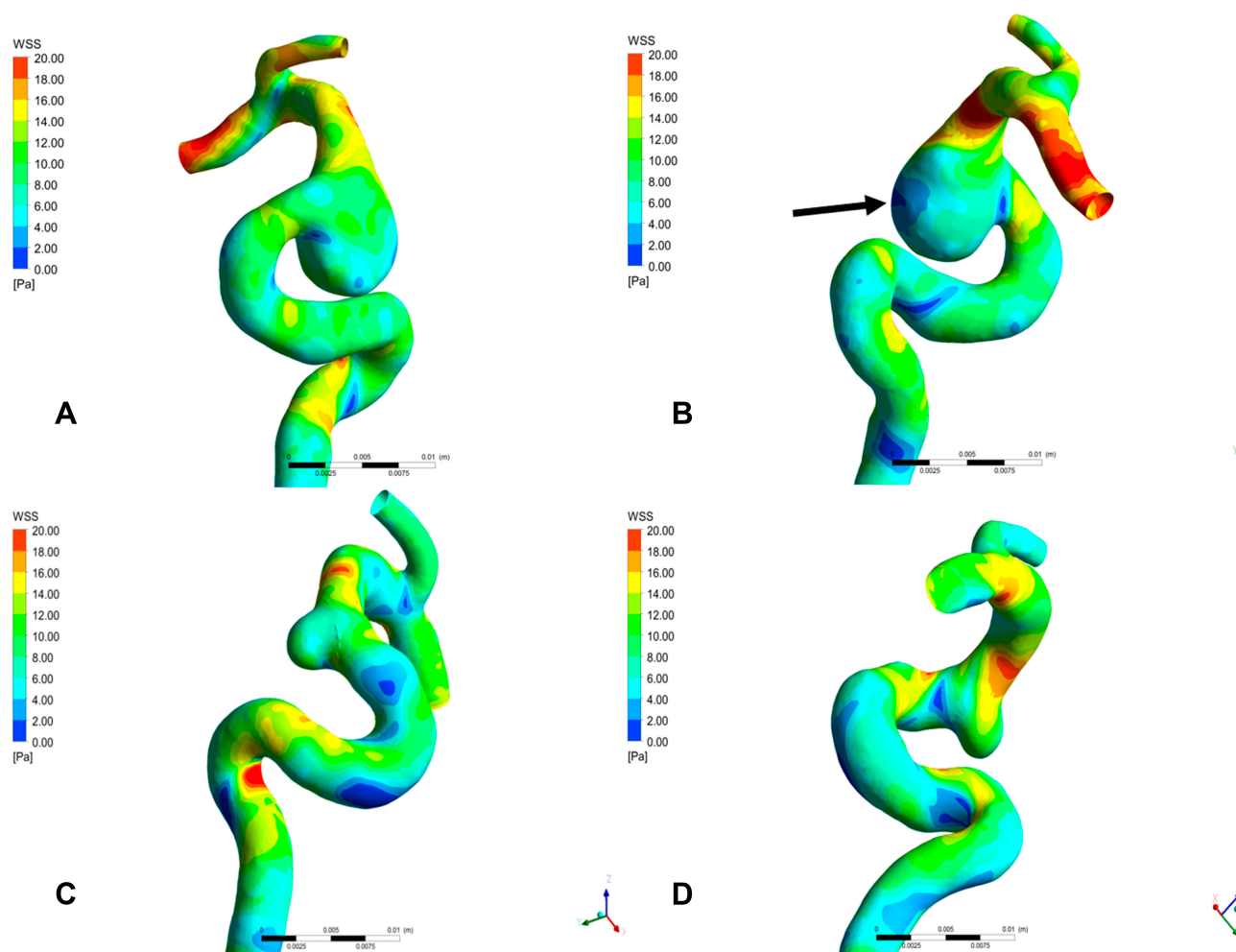


Figure 2 The WSS of the OA-MAN prior to rupture. **(A, B)** WSS of the right ophthalmic artery aneurysm prior to rupture. **(C, D)** WSS of unruptured left ophthalmic artery aneurysm. The WSS of ophthalmic artery aneurysm prior to rupture was significantly lower than that of unruptured left ophthalmic artery aneurysm (arrow).

WSS could lead to atherosclerotic inflammatory infiltration; these inflammatory infiltrates can massively produce matrix metalloproteinases to degrade the extracellular matrix (ECM). Eventually, these lead to aneurysmal rupture.

The morphological characteristics of IAs are associated with hemodynamic parameters. Ujiie et al have argued that higher AR correlates with more complex flow patterns and slower circulation in the aneurysm sac.²⁷ Tremmel et al evaluated the relationship between SR and hemodynamic using a virtual experiment.²⁸ They found that, with increasing SR, the area exposed to low WSS increased. In our study, in addition to NSI, other morphological parameters in pre-ruptured aneurysms were significantly higher than those of unruptured aneurysms, suggesting that larger size and more irregular shape are likely to exist in pre-ruptured aneurysms. The reason why NSI was not statistically significant in our study may be explained by the relatively

small sample size. Lv et al performed a similar study, analyzing morphological characteristics of unruptured posterior communicating artery aneurysms with oculomotor nerve palsy.²⁹ They also found that, comparing the asymptomatic unruptured PComA aneurysms, PComA aneurysms with oculomotor nerve palsy were larger and more irregular in shape. Lower NWSS and higher LSA% were found in the aneurysms prior to rupture.

Limitations

There were some limitations in our study. First, although we compared hemodynamic and morphological characteristics using twelve mirror aneurysms prior to rupture in our study, including seven posterior communicating artery aneurysms, three ophthalmic artery aneurysms and two middle cerebral artery aneurysms, they were located at different locations and their hemodynamics might be different. This might

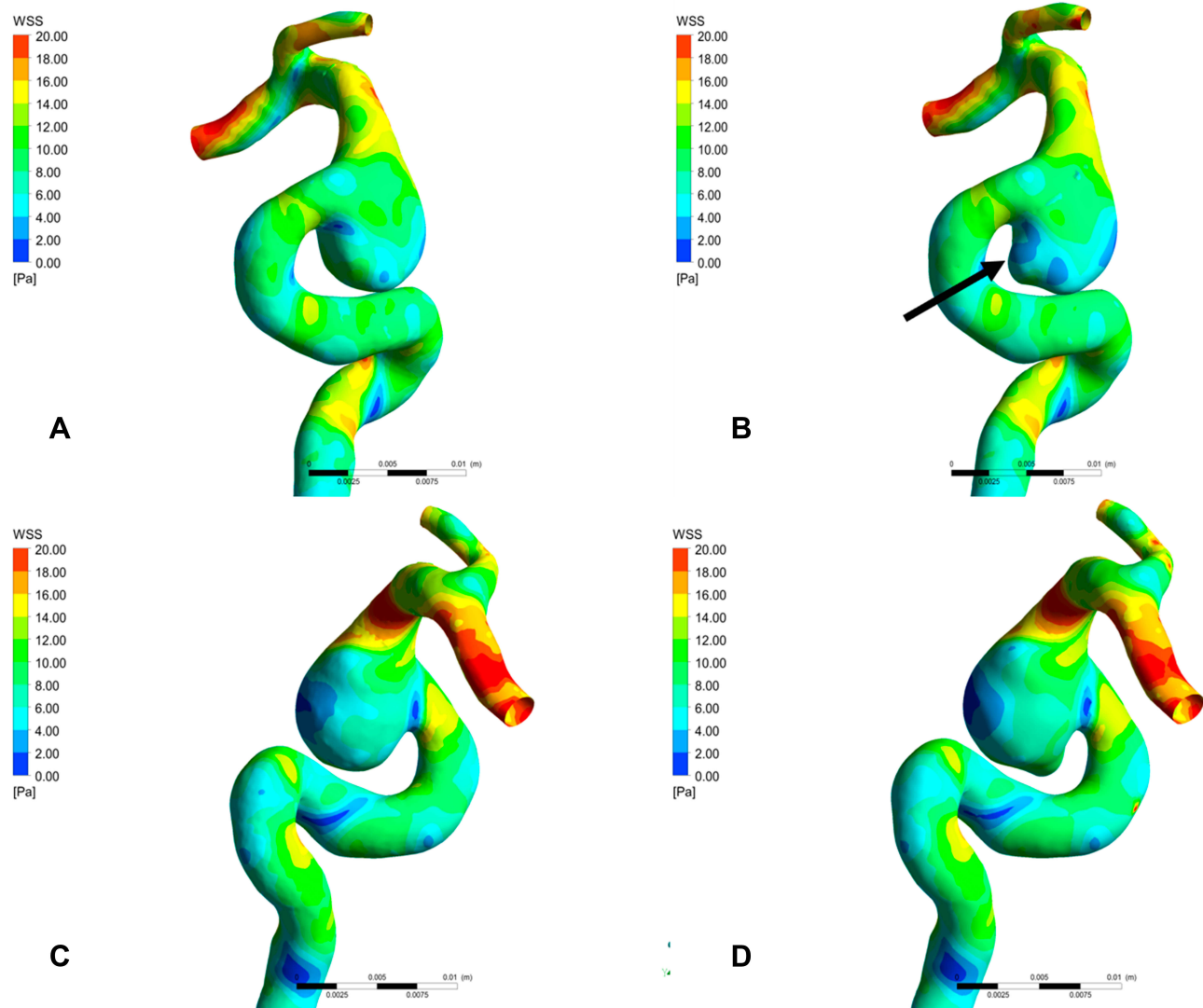


Figure 3 The WSS of the right ophthalmic artery aneurysm prior to rupture. **(A,C)** WSS of the right ophthalmic artery aneurysm before rupture. **(B,D)** WSS of the right ophthalmic artery aneurysm after rupture. The WSS after rupture of the right ophthalmic artery aneurysm is relatively lower than WSS before rupture, especially in the newly generated bleb (arrow).

weaken the accuracy of the results. Further studies using the same location of the mirror aneurysms prior to rupture are needed to confirm our results. Second, to simplify the patient-specific IA models, some small vessel branches distant from the aneurysms were artificially moved. Third, the assumptions of rigid wall, laminar flow, and Newtonian blood flow were used in our patient-specific IA models. To some extent, these treatments might affect the accuracy of the results. Fourth, because the incidence of the MANs was relatively low and the incidence of the MANs prior to rupture was lower still, we need to validate our findings using larger sample sizes from multi-center studies. Finally, for unruptured aneurysms, despite the fact that we believe that three months of follow-up might be sufficient,

IAs might experience growth and rupture in the future. This might have influenced the results.

Conclusions

MANs prior to rupture may be extremely useful models to assess the risk of aneurysm rupture. Larger size, irregular shape, higher AR, SR, UI, NI, and lower WSS were associated with aneurysms prior to rupture. We hope that these results may provide data to guide further studies and provide appropriate treatment strategies.

Acknowledgments

This work was supported by grants from Young and Middle-Aged Natural Science Foundation of Wannan

Medical College (No. WK2018F02), the Nature Science Research Project in Higher Education of Anhui Province's (Nos. KJ2018A0253 and KJ2019A0423) and the Science Research Project of Professional of the First Affiliated Hospital of Wannan Medical College (No. YR201911). Jinlong Yuan and Chenlei Huang are co-first authors for this study.

Author Contributions

All authors made substantial contributions to conception and design, acquisition of data, or analysis and interpretation of data; all took part in drafting the article or revising it critically for important intellectual content; all gave final approval of the version to be published; and agree to be accountable for all aspects of the work.

Disclosure

The authors report no conflicts of interest in this work.

References

- Cebral JR, Mut F, Weir J, et al. Quantitative characterization of the hemodynamic environment in ruptured and unruptured brain aneurysms. *AJNR Am J Neuroradiol.* 2011;32(1):145–151. doi:10.3174/ajnr.A2419
- Metaxa E, Tremmel M, Natarajan SK, et al. Characterization of critical hemodynamics contributing to aneurysmal remodeling at the basilar terminus in a rabbit model. *Stroke.* 2010;43(7):1774–1782. doi:10.1161/STROKEAHA.110.585992
- Sugiyama S, Meng H, Funamoto K, et al. Hemodynamic analysis of growing intracranial aneurysms arising from a posterior inferior cerebellar artery. *World Neurosurg.* 2012;78(5):462–468. doi:10.1016/j.wneu.2011.09.023
- Xiang J, Natarajan SK, Tremmel M, et al. Hemodynamic-morphologic discriminants for intracranial aneurysm rupture. *Stroke.* 2011;42(1):144–152. doi:10.1161/strokeaha.110.592923
- Cebral JR, Castro MA, Appanaboyina S, Putman CM, Millan D, Frangi AF. Efficient pipeline for image-based patient-specific analysis of cerebral aneurysm hemodynamics: technique and sensitivity. *IEEE Trans Med Imaging.* 2005;24(4):457–467. doi:10.1109/tmi.2005.844159
- Lu G, Huang L, Zhang XL, et al. Influence of hemodynamic factors on rupture of intracranial aneurysms: patient-specific 3d mirror aneurysms model computational fluid dynamics simulation. *AJNR Am J Neuroradiol.* 2011;32(7):1255–1261. doi:10.3174/ajnr.A2461
- Xu J, Yu Y, Wu X, et al. Morphological and hemodynamic analysis of mirror posterior communicating artery aneurysms. *PLoS One.* 2013;8(1):e55413. doi:10.1371/journal.pone.0055413
- Fan J, Wang Y, Liu J, et al. Morphological-hemodynamic characteristics of intracranial bifurcation mirror aneurysms. *World Neurosurg.* 2015;84(1):114–120 e112. doi:10.1016/j.wneu.2015.02.038
- Wang GX, Liu J, Chen YQ, et al. Morphological characteristics associated with the rupture risk of mirror posterior communicating artery aneurysms. *J Neurointerv Surg.* 2018;10(10):995–998. doi:10.1136/neurintsurg-2017-013553
- Kono K, Tomura N, Yoshimura R, Terada T. Changes in wall shear stress magnitude after aneurysm rupture. *Acta Neurochir (Wien).* 2013;155(8):1559–1563. doi:10.1007/s00701-013-1773-2
- Sforza DM, Putman CM, Scrivano E, Lylyk P, Cebral JR. Blood-flow characteristics in a terminal basilar tip aneurysm prior to its fatal rupture. *AJNR Am J Neuroradiol.* 2010;31(6):1127–1131. doi:10.3174/ajnr.A2021
- Cebral JR, Hendrickson S, Putman CM. Hemodynamics in a lethal basilar artery aneurysm just before its rupture. *AJNR Am J Neuroradiol.* 2009;30(1):95–98. doi:10.3174/ajnr.A1312
- Valencia A, Burdiles P, Ignat M, et al. Fluid structural analysis of human cerebral aneurysm using their own wall mechanical properties. *Comput Math Methods Med.* 2013;2013:293128. doi:10.1155/2013/293128
- Cebral JR, Mut F, Raschi M, et al. Aneurysm rupture following treatment with flow-diverting stents: computational hemodynamics analysis of treatment. *AJNR Am J Neuroradiol.* 2011;32(1):27–33. doi:10.3174/ajnr.A2398
- Jou LD, Lee DH, Morsi H, Mawad ME. Wall shear stress on ruptured and unruptured intracranial aneurysms at the internal carotid artery. *AJNR Am J Neuroradiol.* 2008;29(9):1761–1767. doi:10.3174/ajnr.A1180
- Liu J, Xiang J, Zhang Y, et al. Morphologic and hemodynamic analysis of paraclinoid aneurysms: ruptured versus unruptured. *J Neurointerv Surg.* 2014;6(9):658–663. doi:10.1136/neurintsurg-2013-010946
- Backes D, Vergouwen MD, Velthuis BK, et al. Difference in aneurysm characteristics between ruptured and unruptured aneurysms in patients with multiple intracranial aneurysms. *Stroke.* 2014;45(5):1299–1303. doi:10.1161/strokeaha.113.004421
- Dhar S, Tremmel M, Mocco J, et al. Morphology parameters for intracranial aneurysm rupture risk assessment. *Neurosurg.* 2008;63(2):185–196. doi:10.1227/01.NEU.0000316847.64140.81
- Scholtes F, Martin D. Strategic implications of aneurysmal cranial nerve compression. *Neurochirurgie.* 2012;58(2–3):146–155. doi:10.1016/j.neuchi.2012.02.019
- Langner S, Schroeder HW, Hosten N, Kirsch M. Diagnosing neurovascular compression syndromes. *Rofo.* 2012;118(3):220–228. doi:10.1055/s-0031-1281976
- Hodis S, Uthamaraj S, Lanzino G, et al. Computational fluid dynamics simulation of an anterior communicating artery ruptured during angiography. *J Neurointerv Surg.* 2014;6(2):e14. doi:10.1136/neurintsurg-2012-010596
- Pereira VM, Brina O, Bijlenga P, et al. Wall shear stress distribution of small aneurysms prone to rupture: a case-control study. *Stroke.* 2014;45(1):261–264. doi:10.1161/strokeaha.113.003247
- Liu J, Fan J, Xiang J, Zhang Y, Yang X. Hemodynamic characteristics of large unruptured internal carotid artery aneurysms prior to rupture: a case control study. *J Neurointerv Surg.* 2016;8(4):367–372. doi:10.1136/neurintsurg-2014-011577
- Duan G, Lv N, Yin J, et al. Morphological and hemodynamic analysis of posterior communicating artery aneurysms prone to rupture: a matched case-control study. *J Neurointerv Surg.* 2016;8(1):47–51. doi:10.1136/neurintsurg-2014-011450
- Casimiro MV, McEvoy AW, Watkins LD, Kitchen ND. A comparison of risk factors in the etiology of mirror and non-mirror multiple intracranial aneurysms. *Surg Neurol.* 2004;61(6):541–545. doi:10.1016/j.surneu.2003.08.016
- Juvela S. Risk factors for multiple intracranial aneurysms. *Stroke.* 2000;31(2):392–397. doi:10.1161/01.str.31.2.392
- Ujiiie H, Tachibana H, Hiramatsu O, et al. Effects of size and shape (aspect ratio) on the hemodynamics of saccular aneurysms: a possible index for surgical treatment of intracranial aneurysms. *Neurosurg.* 1999;45(1):119–129. doi:10.1097/00006123-199907000-00028
- Tremmel M, Dhar S, Levy EI, Mocco J, Meng H. Influence of intracranial aneurysm-to-parent vessel size ratio on hemodynamics and implication for rupture: results from a virtual experimental study. *Neurosurg.* 2009;64(4):622–630. doi:10.1227/01.NEU.0000341529.11231.69
- Lv N, Yu Y, Xu J, Karmonik C, Liu J, Huang Q. Hemodynamic and morphological characteristics of unruptured posterior communicating artery aneurysms with oculomotor nerve palsy. *J Neurosurg.* 2016;125(2):264–268. doi:10.3171/2015.6.JNS15267

Neuropsychiatric Disease and Treatment

Dovepress

Publish your work in this journal

Neuropsychiatric Disease and Treatment is an international, peer-reviewed journal of clinical therapeutics and pharmacology focusing on concise rapid reporting of clinical or pre-clinical studies on a range of neuropsychiatric and neurological disorders. This journal is indexed on PubMed Central, the 'PsycINFO' database and CAS, and

is the official journal of The International Neuropsychiatric Association (INA). The manuscript management system is completely online and includes a very quick and fair peer-review system, which is all easy to use. Visit <http://www.dovepress.com/testimonials.php> to read real quotes from published authors.

Submit your manuscript here: <https://www.dovepress.com/neuropsychiatric-disease-and-treatment-journal>